GeoHazards

MDPI

Article

Topographic–Vegetation Interactions on an Incipient Foredune Field Post-Tropical Storm

Jean T. Ellis [1,*], Michelle E. Harris [2] and Brianna F. Barrineau [3]

[1] Department of Geography, University of South Carolina, Columbia, SC 29208, USA
[2] Coastal & Ocean Processes, Virginia Institute of Marine Science, Gloucester Point, VA 23062, USA; mharris@vims.edu
[3] W.K. Dickson & Co., Inc., Columbia, SC 29201, USA
* Correspondence: jtellis@sc.edu

Abstract: Sand dunes protect the most important economic and ecologically critical landscapes from coastal hazards (storms and high-tide flooding). The characteristics of the dune affect their protective ability. This paper qualitatively and quantitatively assesses the relationships between pre- and post-storm conditions for vegetation and the morphology of an incipient dune system along the South Carolina coast. Field-based dune vegetation and morphology measurements were obtained before and after tropical storm Dorian (2019). Vegetation is assessed with respect to distribution and functional type, and subgroups are introduced to categorize land cover transitions. At the quadrat scale (0.2 m^2) following the storm, there was a shift from stabilizer to builder, a decrease of sand (2%), and the vegetation remained consistent at around 61% of the land cover. Transect-level analysis (0.2 m × 1.0 m) revealed distinct variability concerning post-storm morphology change in the extreme study site extents. *Dorian* resulted in approximately 10% volumetric loss over the entire study site (101 m^2). This study demonstrated changes to a dune system following a tropical storm with wind as the dominant forcing factor. This study revealed that vegetation presence is not broadly correlated with reduced levels of post-storm erosion.

Keywords: sand dunes; tropical cyclones; coastal erosion; dune morphology; vegetation; vegetation functional types; incipient foredunes

check for updates

Citation: Ellis, J.T.; Harris, M.E.; Barrineau, B.F. Topographic–Vegetation Interactions on an Incipient Foredune Field Post-Tropical Storm. *GeoHazards* **2024**, *5*, 1207–1219. https://doi.org/10.3390/geohazards5040057

Academic Editor: Zhong Lu

Received: 6 September 2024
Revised: 7 October 2024
Accepted: 25 October 2024
Published: 4 November 2024

Copyright: © 2024 by the authors. Licensee MDPI, Basel, Switzerland. This article is an open access article distributed under the terms and conditions of the Creative Commons Attribution (CC BY) license (https://creativecommons.org/licenses/by/4.0/).

1. Introduction

Sand dunes are economically and ecologically critical to coastal systems [1–4]. They protect residents and infrastructure from coastal hazards, particularly high tide flooding and storm surges. However, tropical cyclones destroy or reduce the integrity of the dune systems [5–8]. The magnitude of geomorphic change is related to the pre-existing dune morphology [9–12], storm characteristics, and land elevation [13]. Many studies have considered the geomorphic response of dunes to storms, including extratropical systems (e.g., [14,15]). The focus here is those specific to tropical cyclones.

A 7% dune volumetric loss along a 2 km portion of the Florida Panhandle was measured using digital elevation models (DEMs) before and after *Dennis* (2005, [16]). Also, 70% of the incipient foredunes were destroyed along the Florida Panhandle following *Ivan* (2004, [10]). Severe dune erosion was noted along the coast of South Carolina following *Hugo* (1989, [17]). *Dorian* caused 1.7 m^3 m^{-1} of dune erosion along a 1 km stretch of Prince Edward Island [18]. A study on Isle of Palms (IOP), South Carolina, measured 5.9% volumetric gain following *Hugo* [19]. However, that study considered the dune, beach, and nearshore bar system (to −1.5 m MSL) and totaled approximately 250 m of shore perpendicular length. *Irma* resulted in a 39% volumetric dune loss on IOP and along the same dune system, and *Florence* resulted in a 3% volumetric loss [20].

The post-storm recovery of dunes [21–23] is less well documented than that of the beaches [24–26]. However, geomorphic theory suggests that if a storm erodes a primary

foredune, the dune should reform given ideal conditions (adequate sediment supply, wind energy, and cross-shore distance). The interim condition is the formation of an embryo or incipient foredune, which was observed on IOP following *Hugo* (1989, [27]) and *Matthew* (2016, [28]). When considering the before Hurricane *Irma* (2017) to pre-Hurricane *Florence* (2018), the anthropogenic and 'control' dunes lost 15.5% and 40.1% of their volume; the 'control' dunes are in the same geographic location as the incipient dune system studied here [23]. The presence of vegetation is essential to incipient foredune growth, as it provides the structure to trap and store the sand [28–31].

Vegetation is vital to foredune growth, stability, and long-term health [32–37]. Aeolian deposition occurs with 15–20% vegetation coverage in coastal environments [38–42]. Continual burial, vertical growth, and increased soil nutrients create a positive feedback mechanism to encourage additional vegetation establishment, development, and dune stabilization [43,44]. Short-duration studies conclude that vegetation increases foredune height and volume [35] because the wind field is modified and sand accumulates [34,45]. Longer temporal studies (on the scale of weeks) identify a correlation between plant density and sand dune growth [45], thus suggesting vegetation serves as a stabilizing agent.

Plants are characterized according to their morphologic response to dunes. The major functional types are dune builders, burial-tolerant stabilizers, and burial-intolerant stabilizers, with the latter typically found inland of the foredune [46–49]. Dune builders correspond with the vertical growth of dunes, and aboveground biomass serves as a roughness factor that traps wind-blown sand. More extensive and denser vegetation is more successful at increasing dune size and volume. Examples of dune builder species in South Carolina include *Uniola paniculata* (Sea Oats), *Iva imbricata* (Dune Marsh-elder), and *Panicum amarum* (Bitter Panicum). Stabilizing species strengthen the dune and have a smaller surface roughness compared to dune builders. These low-lying species with decumbent growth and dense belowground biomass anchor and stabilize sediment [50]. In South Carolina, typical dune stabilizers include *Ipomoea imperati* (Beach Morning Glory), *Hydrocotyle bonariensis* (Largeleaf Pennywort), and *Oenothera humifusa* (Seabeach Evening Primrose).

Vegetation's role in protecting dunes against erosion is not well-documented, especially in field-based experiments [35,51]. Even less documented is the relationship between increased foredune stability resulting from vegetation present during storm surges (for example, [52]). In a wave tank study that considered three plant species planted on incipient foredunes (they termed embryo coastal dunes), storm-induced erosion was reduced by vegetation presence [53]. The above- and below-ground vegetation components reduced storm surge energetics, reducing erosion [53]. Similar results were observed along a vegetated beach-dune profile with a berm: vegetation impeded landward erosion under large lab-generated wave conditions [54]. Vegetation structure also affects storm surge attenuation [55,56]. A comprehensive study that considered lab and in situ experiments concluded that vegetation provides a 1.6× safety factor over bare sand, which reduces wave run-up erosion of the dunes by 40% [57]. However, after comparing vegetated and bare dunes in a flume, it was stated that coastal managers should "reexamine the predominant paradigm that dune vegetation reduces erosion during extreme events [58]".

This paper aims to qualitatively and quantitatively assess the relationships between pre- and post-storm conditions for vegetation and the morphology of an incipient dune system. The scant literature investigating the linkages between vegetation and dune morphology pre- and post-storm focuses on foredunes; this study examines an incipient foredune system. Vegetation is assessed with respect to distribution and functional type. This paper fills a research need to link vegetation characteristics to the dune's morphologic response from a tropical storm.

1.1. Study Site

Isle of Palms (IOP, Figure 1) is a drumstick barrier island 15.5 km from Charleston, SC, USA. It is a mixed energy coast with semidiurnal tides (1.5 m average range; 2.5 m spring tide range) [59,60]. Annual wave heights average 0.6 m, and 120,000 m^3/yr of fine-grained

quartz sand is transported alongshore from northeast to southwest [61]. The 2018 beach nourishment injected 1.282 million m^3 of sand over approximately 3.8 km of the island's NE portion [62]. The southern extent of this tapered nourishment was about 200 m from the centroid of the study site. Several tropical storms have affected IOP in recent years: *Matthew* (2016), *Irma* (2017), *Florence* (2018), *Michael* (2018), *Dorian* (2019), *Isaias* (2020), *Ian* (2022), *Idalia* (2023), *Debby* (2024), and *Helene* (2024). Accordingly, the storms' impact on IOP dune systems has been extensively documented [20,23,28,63–66].

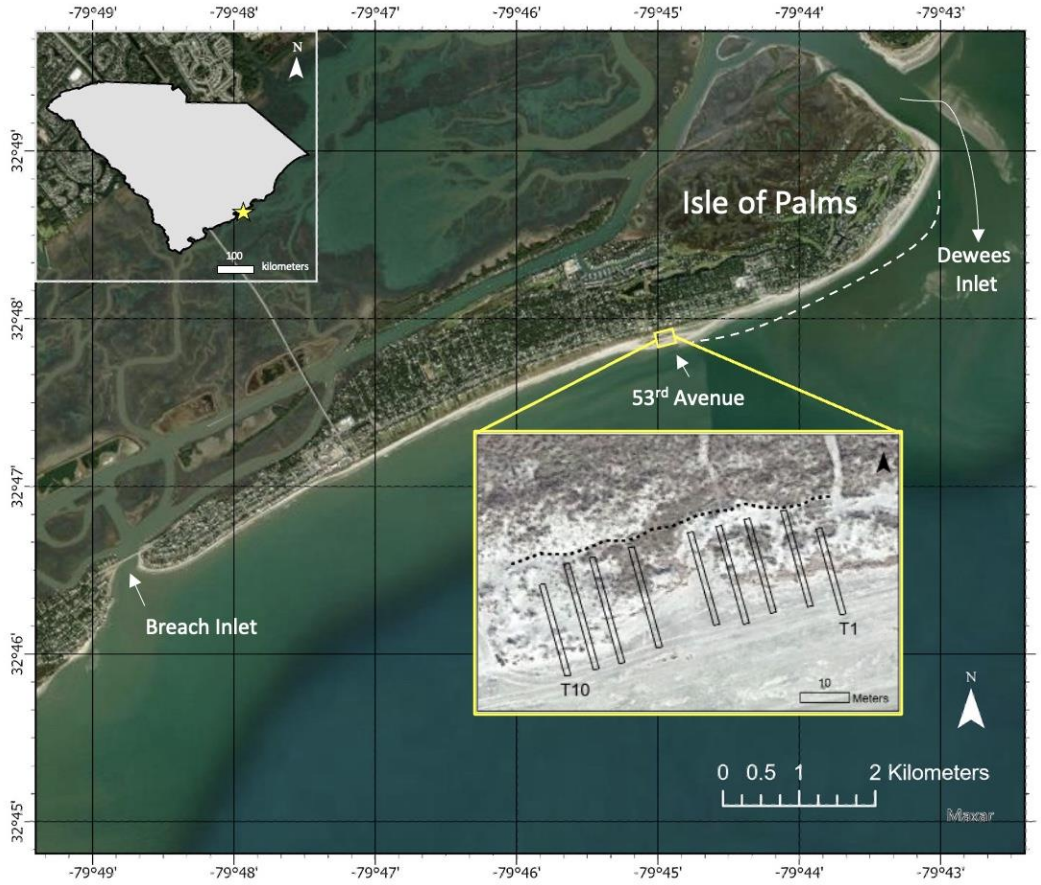


Figure 1. Study site location at 53rd Avenue on Isle of Palms, South Carolina, U.S.A. The topleft panel insert is the State of South Carolina, U.S.A., where the yellow star denotes the location of Isle of Palms (primary image), which is bounded on the northeast and southwest by Dewees and Breach Inlets, respectively. The white dashed line marks the spatial extent of the 2018 beach nourishment. The yellow inset panel denotes the location of 53rd Avenue, where cross-shore transects are presented. The dashed black line is the seaward extent of the developed secondary foredune system. Base imagery: Google Earth Pro (2019), Maxar Technologies.

The study site is 53rd Avenue, three blocks south of a private, gated community. In previous research [28], these dunes were the study's control because of the nominal human impact relative to other U.S. East Coast beach-dune systems. The recent tropical storms have minimally impacted an expansive vegetated backdune system at 53rd Avenue [28]. Before *Matthew*, there was a developed foredune seaward of the vegetated backdune. This area has since been replaced with an incipient foredune field. The 2016 to 2019 annual storms partially prohibited the incipient foredunes from transitioning to a foredune system. Without these storms or excessive (and unexpected) anthropogenic disturbances (such as human trampling), we posit the incipient foredunes would have coalesced into a healthy primary foredune system.

1.2. Forcing Factors

This study is temporally bound by Hurricane *Dorian*, which impacted Charleston, SC (15.5 km from IOP) on 5 September 2019. Geomorphic and land cover data were acquired on 24 August and 8 September 2019 (detailed below). *Dorian* traveled up the east coast of the United States and made landfall in the proximity of the study site on 6 September 2019 near Cape Hatteras, North Carolina (470 km NE of IOP) as a weak Category 2 hurricane with sustained winds of 44 m/s. Before reaching North Carolina, *Dorian* was the second strongest landfalling Atlantic hurricane (Category 5) with sustained winds of 82 m/s [67]. Maximum gusts of 9.9 m/s were measured 2.7 m above the ground (Station 8665530, 16.9 km WSW from IOP, [68]) and 141.0 mm of rainfall (4–5 September, [69]) was measured in Charleston, associated with *Dorian*. *Dorian* arrived during a low tide, contributing to no recorded storm surge in the Charleston region.

The average wind direction was approximately shore parallel (89 degrees at NOAA Station 8665530) during the study period (24 August 2019 and 8 September 2019) [68]. Offshore wave height averaged 1.86 m during the study period (NOAA Station 41004, 69.0 km SE from IOP) [70]. No precipitation was recorded on 24–31 August and 7–8 September (Charleston Air Force Base Station, 29.4 km NW from IOP, [69]). In the days leading up to the storm (1–3 September), 31.3 mm of precipitation was measured (Charleston Air Force Base Station, [69]).

2. Materials and Methods

2.1. Field Methods

The field-based data acquisition comprised topographic and land cover (LC) data collection. Data were acquired on 24 August 2019 and 8 September 2019, representing pre- and post-*Dorian* conditions. Both data types were collected along ten shore-perpendicular transects located 5.5 m apart. The transects started at the seaward extent of the developed secondary foredune system, corresponding with the baseline used by others investigating dunes at the site [23,28] (Figure 1). The seaward transect extent corresponded with the most seaward extent of pre-storm dune vegetation, which also qualitatively aligned with the pre-*Matthew* foredune dune toe line. The transects were numbered 1–10 in a north-to-south direction and spanned 16–24 m (in the shore perpendicular direction). Herein, transects are referred to as "T", for example, transect 1 is T1.

Topographic surveys were conducted using a Sokkia RED-tech II Series 30R Total Station with an instrument accuracy of +/− 2 mm. The total station was located at the approximate midpoint of T6. Data were gathered approximately every meter along the transects and at geomorphic inflection points. Roughly 240 points were acquired for each survey. Ground control points were established using an X90 OPUS Static GPS receiver with a vertical and horizontal accuracy of +/− 5 mm.

LC data were collected by placing a 1.0 m^2 quadrat along the topographic survey transects starting at the seaward extent of the developed secondary foredune system. Vertical photographs at breast height were taken over each quadrat. LC data were not collected along T6 because of the potential damage associated with the total station placement.

2.2. Data Processing Methods

The pre- and post-*Dorian* 1.0 m^2 quadrat photographs showing land cover were digitally subsampled to generate 0.2 m^2 classified LC sections. A supervised approach [64] was used to classify each section according to LC: dune-building species, dune-stabilizing species, sand, wrack, other, or no data. Dune-building or dune-stabilizing species were visually assigned by identifying the most dominant vegetation functional type. Only 0.2 m^2 sections consisting entirely of sand were assigned that designation. For example, 'other' was assigned if the subsampled quadrat was predominately beach detritus, beach litter, or tree debris. 'No data' was assigned when human or technological errors occurred.

The pre- and post-*Dorian* 0.2 m^2 classified LC sections were combined to create 0.2 m × 1.0 m classified LC polygons (Figure 2a). The 1.0 m dimension is aligned in

the shore parallel direction. Each polygon is assigned by determining the dominant LC (sand, stabilizer, builder, wrack, other, or no data) using the 0.2 m^2 classifications.

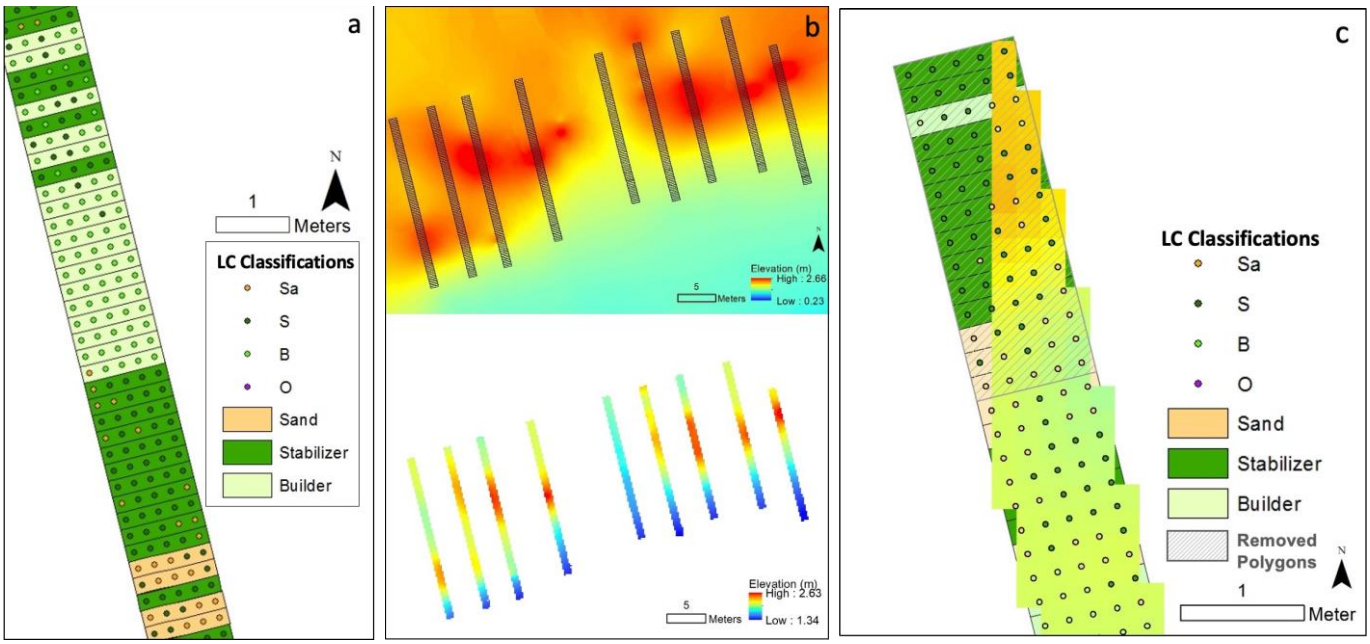


Figure 2. Data processing methods where (**a**) shows the combined pre- and post-Dorian classified LC sections to create 0.2 m × 1.0 m classified polygons; (**b**) is spatially reduced DEMs; and (**c**) shows the polygons considered for analysis. In panels (**a**,**c**): Sa is sand, S is stabilizer, B is builder, and O is other.

The 0.2 m × 1.0 m classified LC polygons were used to conduct a cumulative LC change analysis to compare pre- and post-storm conditions. Four general LC change groups were identified. Subgroup A indicates the LC had no change and was consistently sand. Subgroup B represents a land cover change from vegetation (builder or stabilizer) to sand. The opposite change represents Subgroup C (sand to vegetation). Lastly, Subgroup D is consistently vegetated (stabilizer to builder, builder to stabilizer, always builder, or always stabilizer).

Pre- and post-storm digital elevation models (DEMs) and a DEM-based change map were generated using total station XYZ coordinates and the kriging interpolation method (ArcGIS 10.5.1; cell resolution 0.2 m). The spatial extent of the pre- and post-storm DEM are reduced to align with the 0.2 m × 1.0 m classified LC polygons (Figure 2b). The only polygons considered for analysis are ones where the centroid of all five 0.2 m^2 sections overlap with the DEM (Figure 2c). DEM-based change maps were generated by differencing the pre- and post-storm DEMs.

3. Results

A total of 226 1.0 m^2 quadrat photographs along nine transects were acquired pre- and post-*Dorian*, resulting in 4530 digitally subsampled 0.2 m^2 classified LC sections (Table 1). Sand dominates before and after the storm. There is a post-storm shift in prevalence from stabilizers to builders. Given the minimal prevalence of wrack, other, and no data, these LCs are no longer considered.

Spatial variability of LC was observed across the study site. Figure 3 shows the percentage of sand, stabilizers, and builders for pre- and post-*Dorian* conditions along each transect. According to methods presented in Figure 2, these data are classified as 0.2 m × 1.0 m LC polygons. The most considerable change from *Dorian* occurred along T3 and T8, and the most minor was along T7. At T3, the storm resulted in a 13% increase in sandy surfaces, a 23% loss of stabilizers, and a 9% increase in builders. Regarding the

stabilizers, a similar percent change scenario was observed at T8 (19% loss). Two-thirds of the transects showed decreased sandy surface LC, except for T1–T3.

Table 1. Pre- and post-*Dorian* LC aggregated along T1–T5 and T7–T10 using a 0.2 m^2 resolution. The sum of the LC types is shown in italics.

	Pre-*Dorian*		**Post-*Dorian***	
	Count	**%**	**Count**	**%**
Sand (Sa)	1729	38.2	1637	36.1
Stabilizers (S)	1571	34.7	1308	28.9
Builders (B)	1223	27.0	1511	33.4
Wrack	0	0.0	16	0.4
Other (O)	7	0.2	8	0.2
No data	0	0.0	50	1.1
Sum	*4530*	*100*	*4530*	*100*



Figure 3. Pre- and post-*Dorian* ((**a**,**b**), respectively) percentages of sand, stabilizers, and builders along each transect. Land covers were normalized to 100% for each transect for the pre- and post-storm conditions.

Figure 4 shows pre- and post-*Dorian* LC (a,b) and topographic (c,d) conditions. These LC subgroups (Figure 4) are the classified 0.2 m × 1.0 m LC polygons using the methods to generate data presented in Figure 2. The data in Figure 3a,b are the aggregate data from Figure 4a,b. In Figure 4a,b, the offshore transect extents are consistently sanded except for pre-*Dorian* T2 and post-*Dorian* T4. T7 is consistently and predominantly vegetated (~86%) and T5 is showing the same for sand (~63%) (c.f., Figure 3). The builders appear to be patchier compared to the stabilizers. The DEMs (Figure 4c,d) qualitatively reveal a slight site-level elevation decrease after the storm, particularly toward the southwestern portion of the site (T7–T10). The maximum pre- and post-storm elevations were comparable (2.63 m and 2.59 m), with the minimum elevations calculated at 1.51 m and 1.34 m. There was a calculated volumetric decrease from pre-to post-*Dorian*, measuring 422 and 380 m^3, respectively.

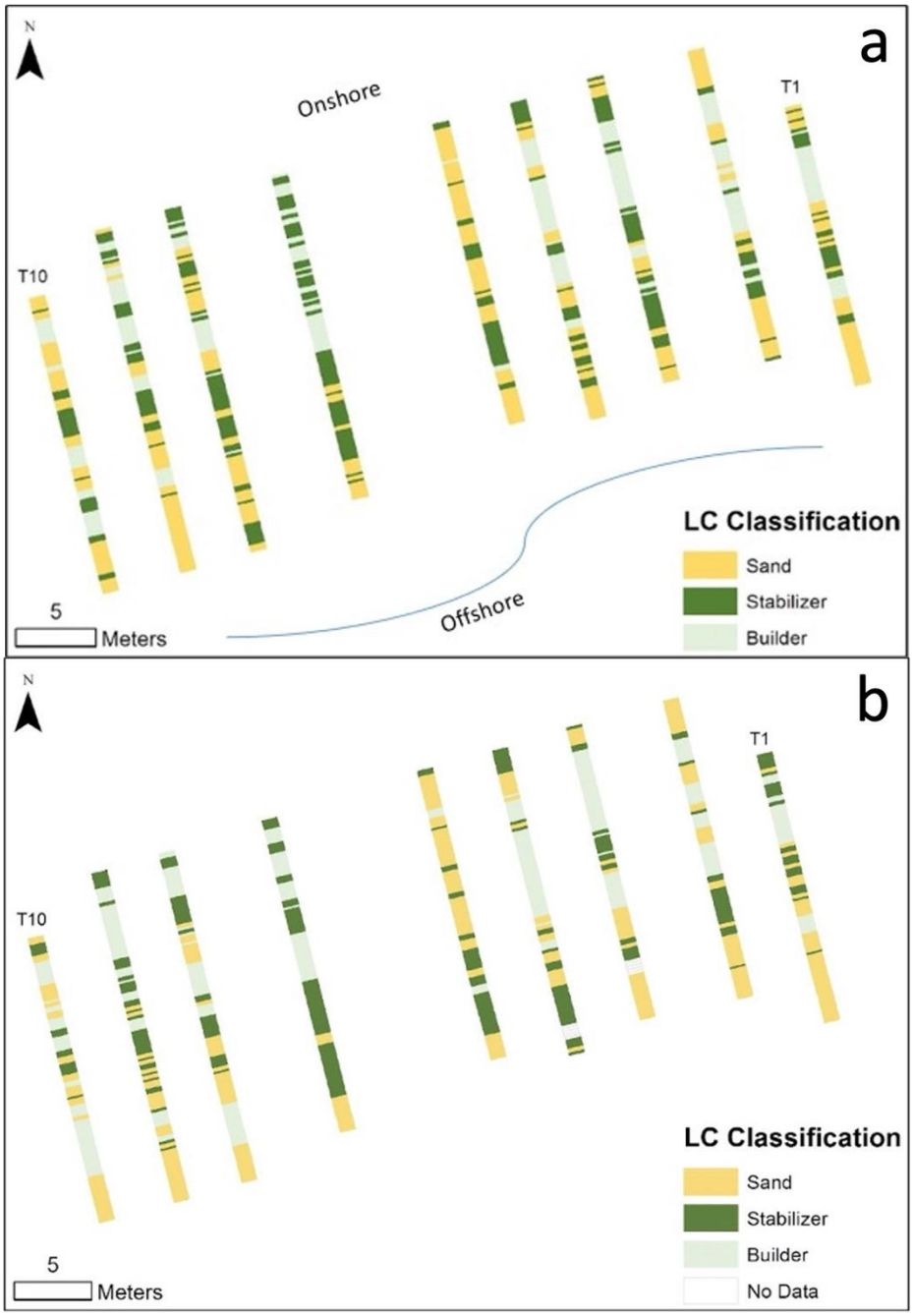


Figure 4. *Cont.*

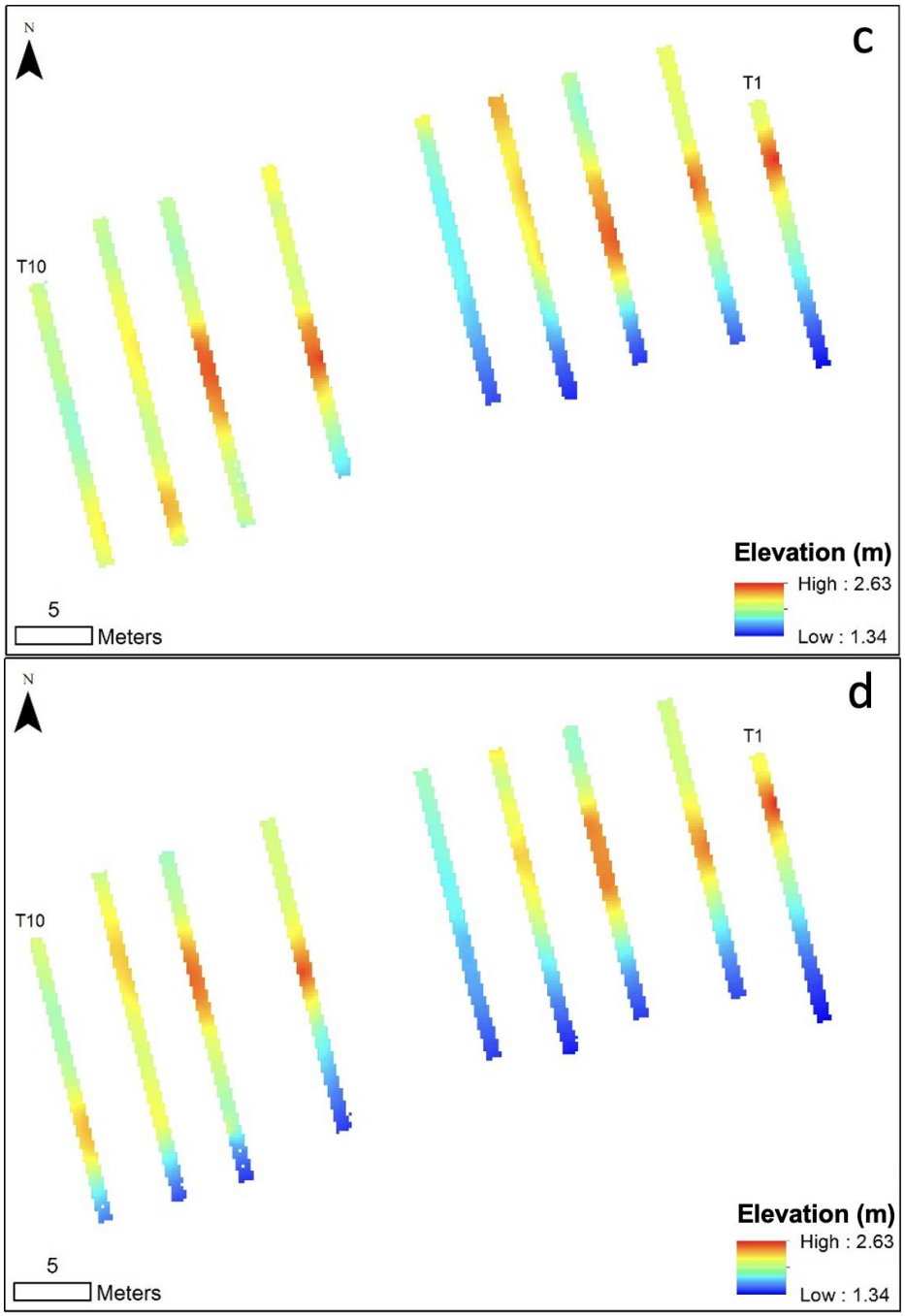


Figure 4. Classified 0.2 m × 1.0 m LC polygons for pre- (**a**) and post- (**b**) Dorian. The pre-and post-*Dorian* DEMs are shown in (**c**,**d**). These results have been clipped to correspond with the methods associated with Figure 2. The offshore and onshore locations shown in (**a**) are the same in (**b**–**d**).

Figure 5 presents the change along each transect from the pre- and post-storm conditions for LC (left) and topography (right). LC change is presented according to subgroup categories, and topography is along a continuum. This figure permits the identification of substantial expanses of continuous LC (according to subgroups) and the description of topographic change for spatially coincident areas. Large patches of Subgroup D (consistent vegetation) were spatially associated with erosion along T1–T4, T6–T7, T9, and T10. Subgroup A (consistent sand) was found in conjunction with strong accretion (T9), slight erosion (T5), or no change (T1). This study did not result in large expanses of Subgroups B or C. When considering all transects, the counts for Subgroups A–D are 212, 116, 117, and 451 (i.e., the data to generate Figure 5). Figure 5 also shows the elevation percent change

(from pre- to post-*Dorian*) for each transect. The southwest portion of the site has a higher percent change, with an average of 9.9%.

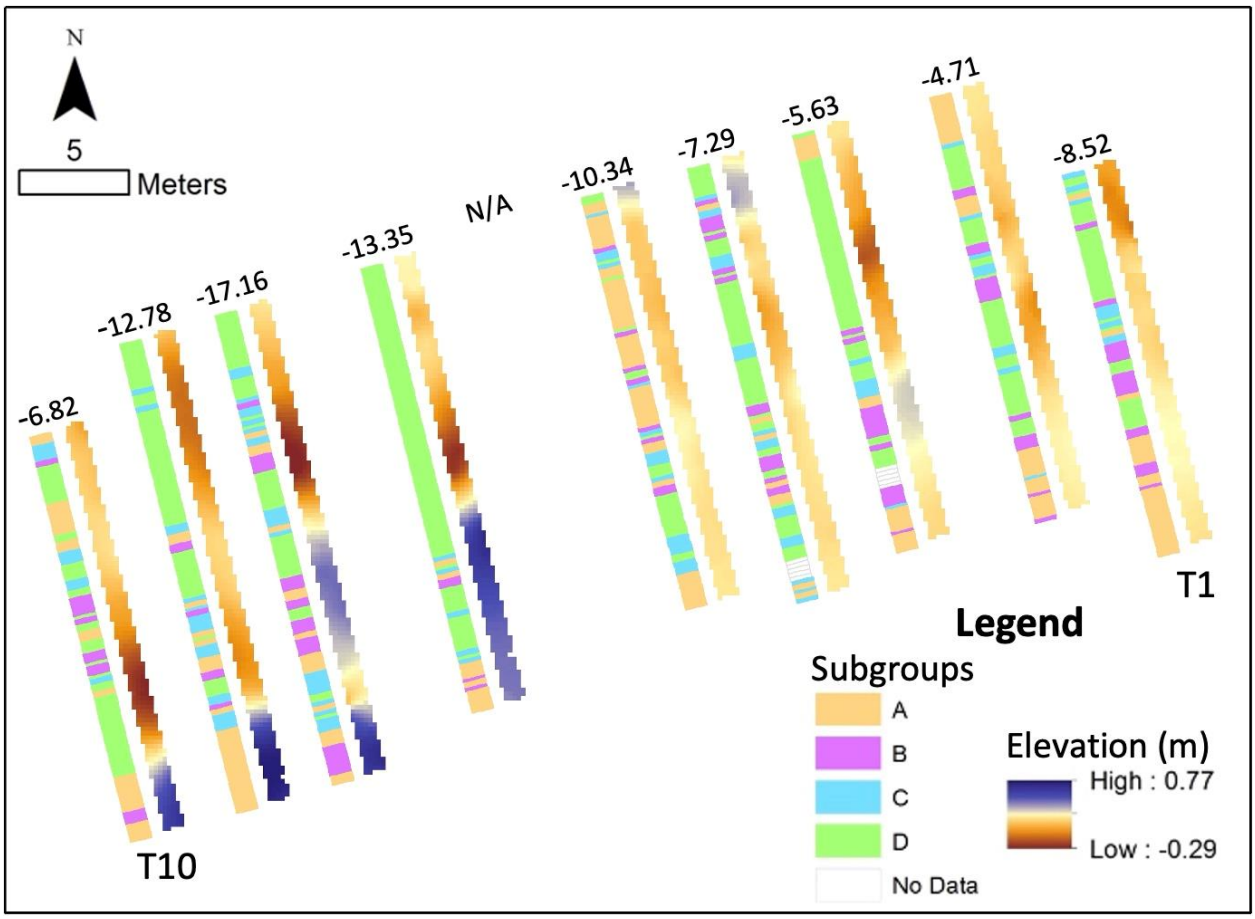


Figure 5. LC Subgroups (left stripes) and DEM (right stripes) change maps for T10 to T1. Numbers indicate the elevation percent change for each transect line.

4. Discussion

Results were presented at two spatial scales—the subsampled quadrat (0.2 m^2; Table 1) and the transect scale (0.2 m × 1.0 m; Figures 3–5). The goal of this research was to qualitatively and quantitatively assess the relationships between pre- and post-storm vegetation conditions and the morphology of an incipient dune system, which is best conducted at the transect scale. As such, the discussion will focus more heavily on this scale. However, Table 1 (the quadrat scale) revealed a shift from stabilizer to builder and a slight decrease of sand (2%), thereby maintaining the vegetation LC at around 61%.

The transect scale figures reveal a separate trend at the northeast and southwest extents of the study site. The southwest transects (T7–T10) showed that the surface deflated offshore where the sand was dominant (situated on the upper backshore, c.f., Figure 1). The most considerable transect level erosion was along T8, T7, and T9. T8 had the largest reduction of stabilizers (44 to 25%) and a substantial increase of builders (18 to 40%).

The northeast extent (T1–T3) of the study site was the only region that did not deflate due to *Dorian*. The *Dorian* storm characteristics, with minimal to no storm surge, strongly suggest that the changes presented in Figure 3 result from aeolian forcing factors.

The storm resulted in approximately 10% volumetric loss over 101 m^2, a relatively small area. Figure 6 shows the relationships between elevation and land cover subgroup change over time. Previous research [10] suggests storms transition LC from vegetation to sand; however, subgroups were not explicitly employed. This study revealed the opposite. The least dominant change was vegetation to sand (Subgroup B, Figure 6). The qualitative

observations that vegetation was not uprooted or buried by sand are likely related to the timing of *Dorian*'s impact, which resulted in no storm surge. Additionally, more than half of all the LC change was from one vegetation type to a second vegetation type or had no vegetation 'type' change (Subgroup D, Figure 6), demonstrating the vegetation's robustness against *Dorian*'s strength.

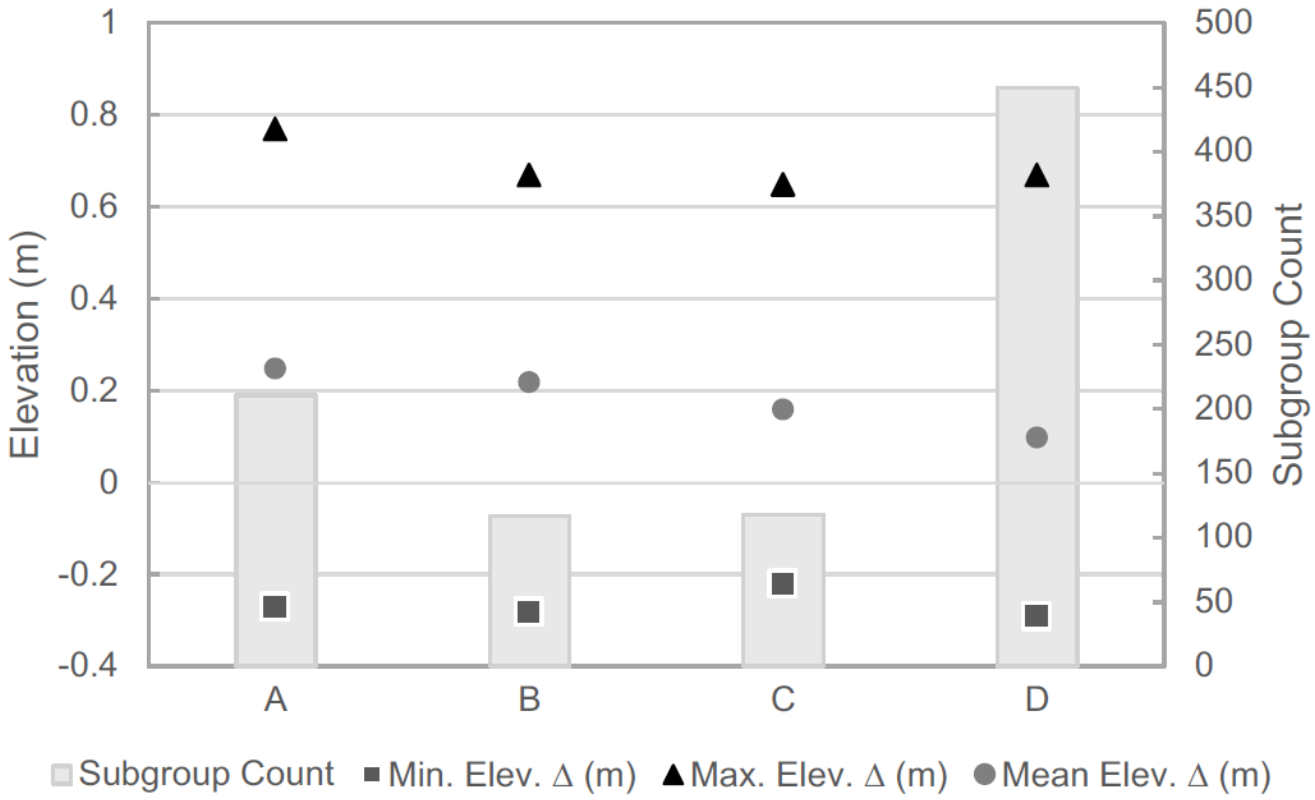


Figure 6. Elevation change and count according to subgroup.

There appears to be an inconsistent pattern related to post-storm elevation change and pre-storm LC (Figure 6). The most extreme minimum and maximum elevation changes were associated with Subgroups A and C, which were sand before *Dorian*.

This research demonstrated the importance of spatial scale when investigating geomorphic change. The subsampled quadrat scale revealed slightly different relationships compared to the transect scale. However, no distinct spatial relationships were established between stabilizers and builders. This work introduced the concept of subgroups, and it is suggested that it be employed in future studies. Results from previous lab- and field-based studies [16–18,21,23,28] compared to those from this one illuminate the importance of continued research on the impact of tropical cyclones on coastal dunes. Results from this study appear to be strongly interdependent with *Dorian* having a weak storm surge, which speaks further to the importance of multiple studies to diversify the types of storms and beach systems under investigation. These findings support recent lab-based work from [58] that vegetation is not broadly correlated with reduced levels of post-storm erosion.

Author Contributions: Conceptualization, J.T.E., B.F.B. and M.E.H.; methodology, J.T.E., M.E.H. and B.F.B.; formal analysis, M.E.H., B.F.B. and J.T.E.; resources, J.T.E.; data curation, M.E.H. and B.F.B.; writing—original draft preparation, J.T.E.; writing—review and editing, J.T.E., M.E.H. and B.F.B.; visualization, M.E.H. and J.T.E.; supervision, J.T.E.; project administration, J.T.E.; funding acquisition, J.T.E. All authors have read and agreed to the published version of the manuscript.

Funding: Financial support was received from the USC Department of Geography and USC's HVRI.

Data Availability Statement: The raw data supporting the conclusions of this article will be made available by the authors on request.

Acknowledgments: Patrick Barrineau and Peter Tereszkiewicz assisted with field-based data collection. The authors thank ALE and PPC, especially Monty Creosote, for their support.

Conflicts of Interest: Author Brianna F. Barrineau was employed by the company W.K. Dickson & Co., Inc. The remaining authors declare that the research was conducted in the absence of any commercial or financial relationships that could be construed as a potential conflict of interest.

References

1. DeGroot, R.S.; Wilson, M.A.; Boumans, R.M.J. A Typology for the Classification, Description, and Valuation of Ecosystem Functions, Goods, and Services. *Ecol. Econ.* **2002**, *41*, 393–408. [CrossRef]
2. Natural Research Council. *Valuing Ecosystem Services: Toward Better Environmental Decision-Making*; National Academies Press: Washington, DC, USA, 2005; 277p.
3. Martinez, M.L.; Hesp, P.A.; Gallego-Fernández, J.B. Coastal Dunes: Human Impact and Need for Restoration. In *Restoration of Coastal Dunes*; Martinez, M.L., Gallego-Fernández, J.B., Hesp, P.A., Eds.; Springer: Berlin/Heidelberg, Germany, 2013; pp. 1–14.
4. Elko, N.; Brodie, K.; Stockton, H.; Nordstrom, K.; Houser, C.; McKenna, K.; Moore, L.; Rosati, J.; Ruggiero, P.; Thuman, R.; et al. Dune Management Challenges on Developed Coasts. *Shore Beach* **2016**, *84*, 15–28.
5. Coco, G.; Senechal, N.; Rejas, A.; Bryan, K.R.; Capo, S.; Parisot, J.P.; Brown, J.A.; MacMahan, J.H.M. Beach Response to a Sequence of Extreme Storms. *Geomorphology* **2014**, *204*, 493–501. [CrossRef]
6. Karunarathna, H.; Pender, D.; Ranasinghe, R.; Short, A.D.; Reeve, D.E. The Effects of Storm Clustering on Beach Profile Variability. *Mar. Geol.* **2014**, *348*, 103–112. [CrossRef]
7. Dissanayake, P.; Brown, J.; Wisse, P.; Karunarathna, H. Effect of Storm Clustering on Beach/Dune Erosion. *J. Geol.* **2015**, *370*, 63–75.
8. Angnuureng, D.B.; Almar, R.; Senechal, N.; Castelle, B.; Addo, K.A.; Marieu, V.; Ranasinghe, R. Shoreline Resilience to Individual Storms and Storm Clusters on a Meso-Macrotidal Barred Beach. *Geomorphology* **2017**, *290*, 265–276. [CrossRef]
9. Hall, M.J.; Halsey, S.D. Comparison of Overwash Penetration from Hurricane Hugo and Pre-Storm Erosion Rates for Myrtle Beach and North Myrtle Beach, South Carolina, USA. *J. Coast. Res.* **1991**, *SI8*, 229–235.
10. Claudino-Sales, V.; Wang, P.; Horwitz, M.H. Factors Controlling the Survival of Coastal Dunes during Multiple Hurricane Impacts in 2004 and 2005: Santa Rosa Barrier Island, Florida. *Geomorphology* **2008**, *95*, 295–315. [CrossRef]
11. Plant, N.G.; Stockdon, H.F. Probabilistic Prediction of Barrier-Island Response to Hurricanes. *J. Geophys. Res. Earth Surf.* **2012**, *117*, F03015. [CrossRef]
12. Houser, C.; Wernette, P.; Rentschlar, E.; Jones, H.; Hammond, B.; Trimble, S. Post-Storm Beach and Dune Recovery: Implications for Barrier Island Resilience. *Geomorphology* **2015**, *234*, 54–63. [CrossRef]
13. Morton, R.A. Factors Controlling Storm Impacts on Coastal Barriers and Beaches—A Preliminary Basis for Near Real-Time Forecasting. *J. Coast. Res.* **2002**, *18*, 486–501.
14. Cheng, J.; Cossu, F.T.; Wang, P. Factors Controlling Longshore Variations of Beach Changes Induced by Tropical Storm Eta (2020) along Pinellas County Beaches, West-Central Florida. *Shore Beach* **2021**, *89*, 75–85. [CrossRef]
15. Burvingt, O.; Castelle, B. Storm Response and Multi-Annual Recovery of Eight Coastal Dunes Spread along the Atlantic Coast of Europe. *Geomorphology* **2023**, *435*, 108735. [CrossRef]
16. Priestas, A.M.; Fagherazzi, S. Morphological Barrier Island Changes and Recovery of Dunes after Hurricane Dennis, St. George Island, Florida. *Geomorphology* **2010**, *114*, 614–626. [CrossRef]
17. Coch, N.K.; Wolff, M.P. Effects of Hurricane Hugo Storm Surge in Coastal South Carolina. *J. Coast. Res.* **1991**, *SI8*, 201–226.
18. George, E.; Lunardi, B.; Smith, A.; Lehner, J.; Wernette, P.; Houser, C. Short Communication: Storm Impact and Recovery of a Beach-Dune System in Prince Edward Island. *Geomorphology* **2021**, *384*, 107721. [CrossRef]
19. Katuna, M.P. The Effect of Hurricane Hugo on the Isle of Palms, South Carolina: From Destruction to Recovery. *J. Coast. Res.* **1991**, *SI8*, 263–273.
20. Ellis, J.T.; Harris, M.E.; Román-Rivera, M.A.; Ferguson, J.B.; Tereszkiewicz, P.A.; McGill, S.P. Application of the Saffir-Simpson Hurricane Wind Scale to Assess Sand Dune Response to Tropical Storms. *J. Mar. Sci. Eng.* **2020**, *8*, 670. [CrossRef]
21. Héquette, A.; Ruz, M.H.; Zemmour, A.; Marin, D.; Cartier, A.; Sipka, V. Alongshore Variability in Coastal Dune Erosion and Post-Storm Recovery, Northern Coast of France. *J. Coast. Res.* **2019**, *SI88*, 25–45. [CrossRef]
22. Davidson, S.G.; Hesp, P.A.; Miot de Silva, G. Controls on Dune Scarping Controls. *Prog. Phys.Geogr.* **2020**, *125*. [CrossRef]
23. Ellis, J.T.; Román-Rivera, M.A.; Harris, M.E.; Tereszkiewicz, P.A. Two Years and Two Hurricanes Later: Did the Dunes Recover? *Shore Beach* **2020**, *88*, 3–12. [CrossRef]
24. Zhang, K.; Douglas, B.; Leatherman, S.; July, N.; Zhang, K. Do Storms Cause Long-Term Beach Erosion along the U.S. East Barrier Coast? *J. Geol.* **2002**, *110*, 493–502. [CrossRef]
25. McKenna, K.; Farrell, S.; Gebert, J. Hurricane Sandy: Beach-Dune Performance at New Jersey Beach Profile Network Sites. *Shore Beach* **2014**, *82*, 13–23.

26. Masselink, G.; Scott, T.; Poate, T.; Russell, P.; Davidson, M.; Conley, D. The Extreme 2013/2014 Winter Storms: Hydrodynamic Forcing and Coastal Response along the Southwest Coast of England. *Earth Surf. Process. Landf.* **2016**, *41*, 378–391. [CrossRef]
27. Sexton, W.J.; Hayes, M.O. The Geologic Impact of Hurricane Hugo and Post-Storm Shoreline Recovery along the Undeveloped Coastline of South Carolina, Dewees Island to the Santee Delta. *J. Coast. Res.* **1991**, *SI8*, 275–290.
28. Ellis, J.T.; Román-Rivera, M.A. Assessing Natural and Mechanical Dune Performance in a Post-Hurricane Environment. *J. Mar. Sci. Eng.* **2019**, *7*, 126. [CrossRef]
29. McGuirk, M.T.; Kennedy, D.M.; Konlechner, T.; Chiaradia, A. Quantifying Changes in Surface Elevation in Conjunction with Growth Characteristics of Incipient and Foredune Vegetation. *J. Coast. Res.* **2021**, *37*, 216–224. [CrossRef]
30. McGuirk, M.T.; Kennedy, D.M.; Konlechner, T. The Role of Vegetation in Incipient Dune and Foredune Development and Morphology: A Review. *J. Coast. Res.* **2022**, *38*, 414–428. [CrossRef]
31. Derijckere, J.; Strypsteen, G.; Rauwoens, P. Early-Stage Development of an Artificial Dune with Varying Plant Density and Distribution. *Geomorphology* **2023**, *437*, 108806. [CrossRef]
32. Hesp, P.A. A Review of Biological and Geomorphological Processes Involved in the Initiation and Development of Incipient Foredunes. *Proc. R. Soc. Edinb.* **1989**, *96B*, 181–201. [CrossRef]
33. De Vries, S.; Southgate, H.N.; Kanning, W.; Ranasinghe, R. Dune Behavior and Aeolian Transport on Decadal Timescales. *Coast. Eng.* **2012**, *67*, 41–53. [CrossRef]
34. Durán, O.; Moore, L.J. Vegetation Controls on the Maximum Size of Coastal Dunes. *Proc. Natl. Acad. Sci. USA* **2013**, *110*, 17217–17222. [CrossRef] [PubMed]
35. Feagin, R.A.; Figlus, J.; Zinnert, J.C.; Sigren, J.; Martínez, M.L.; Silva, R.; Smith, W.K.; Cox, D.; Young, D.R.; Carter, G. Going with the Flow or Against the Grain? The Promise of Vegetation for Protecting Beaches, Dunes, and Barrier Islands from Erosion. *Front. Ecol. Environ.* **2015**, *13*, 203–210. [CrossRef]
36. Keijsers, J.G.S.; De Groot, A.V.; Riksen, M.J.P.M. Modeling the Biogeomorphic Evolution of Coastal Dunes in Response to Climate Change. *J. Geophys. Res. Earth* **2016**, *121*, 1161–1181. [CrossRef]
37. Delgado-Fernandez, I.; O'Keeffe, N.; Davidson-Arnott, R.G.D. Natural and Human Controls on Dune Vegetation Cover and Disturbance. *Sci. Total Environ.* **2019**, *672*, 643–656. [CrossRef] [PubMed]
38. Zhang, L.; Baas, A.C.W. Mapping Functional Vegetation Abundance in a Coastal Dune Environment Using a Combination of LSMA and MLC: A Case Study at Kenfig NNR, Wales. *Int. J. Remote Sens.* **2012**, *33*, 5043–5071. [CrossRef]
39. Lancaster, N.; Baas, A. Influence of Vegetation Cover on Sand Transport by Wind: Field Studies at Owens Lake, California. *Earth Surf. Process. Landf.* **1998**, *23*, 69–82. [CrossRef]
40. Leenders, J.K.; Sterk, G.; Van Boxel, J.H. Modelling Wind-Blown Sediment Transport Around Single Vegetation Elements. *Earth Surf. Process. Landf.* **2011**, *36*, 1218–1229. [CrossRef]
41. Pelletier, J.D.; Mitasova, H.; Harmon, R.S.; Overton, M. The Effects of Interdune Vegetation Changes on Eolian Dune Field Evolution: A Numerical-Modeling Case Study at Jockey's Ridge, North Carolina, USA. *Earth Surf. Process. Landf.* **2009**, *34*, 1245–1254. [CrossRef]
42. Nickling, W.G.; Neuman, C.M. Aeolian Sediment Transport. In *Geomorphology of Desert Environments*; Springer: Dordrecht, The Netherlands, 2009; pp. 517–555.
43. Acosta, A.; Ercole, S.; Stanisci, A.; de Patta Pillar, V.; Blasi, C. Coastal Vegetation Zonation and Dune Morphology in Some Mediterranean Ecosystems. *J. Coast. Res.* **2007**, *23*, 1518–1524. [CrossRef]
44. Acosta, A.; Carranza, M.L.; Izzi, C.F. Combining Land Cover Mapping of Coastal Dunes with Vegetation Analysis. *Appl. Veg. Sci.* **2005**, *8*, 133–138. [CrossRef]
45. Hesp, P.A. *Eolian Sediments and Processes*; Elsevier Science Publishers, B.V.: Amsterdam, The Netherlands, 1983; pp. 325–342.
46. Hosier, P.E. The Effects of Oceanic Overwash on the Vegetation of Core and Shackleford Banks, North Carolina. Ph.D. Dissertation, Duke University, Durham, NC, USA, 1974; p. 3206.
47. Woodhouse, W.W., Jr. *Coastal Sand Dunes of the United States: A Brief Review of Their Importance, Factors Affecting Their Formation and Management Considerations*; U.S. Army Corps of Engineers, Coastal Engineering Research Center: Fort Belvoir, VA, USA, 1982.
48. Ehrenfeld, J.G. Dynamics and Processes of Barrier-Island Vegetation. *Rev. Aquat. Sci.* **1990**, *2*, 437–480.
49. Stallins, J.A. Stability Domains in Barrier Island Dune Systems. *Ecol. Complex.* **2005**, *2*, 410–430. [CrossRef]
50. Bryant, D.B.; Bryant, M.A.; Grzegorzewski, A.S. *Erosion of Coastal Foredunes: A Review on the Effect of Dune Vegetation*; U.S. Army Corps of Engineers Publication #ERDC/CHL CHETN-I-94: Vicksburg, MS, USA, 2017. [CrossRef]
51. Sigren, J.M.; Figlus, J.; Armitage, A.R. Coastal sand dunes and dune vegetation: Restoration, erosion, and storm protection. *Shore Beach* **2014**, *82*, 5–12.
52. Charbonneau, B.R.; Wootton, L.S.; Wnek, J.P.; Langley, J.A.; Posner, M.A. A species effect on storm erosion: Invasive sedge stabilized dunes more than native grass during Hurricane Sandy. *J. Appl. Ecol.* **2017**, *54*, 1385–1394. [CrossRef]
53. Maximiliano-Cordova, C.; Salgado, K.; Martínez, M.L.; Mendoza, E.; Silva, R.; Guevara, R.; Feagin, R.A. Does the functional richness of plants reduce wave erosion on embryo coastal dunes? *Estuaries Coasts* **2019**, *42*, 1730–1741. [CrossRef]
54. Silva, R.; Martínez, M.L.; Odériz, I.; Mendoza, E.; Feagin, R.A. Response of vegetated dune–beach systems to storm conditions. *Coast. Eng.* **2016**, *109*, 53–62. [CrossRef]
55. Mendoza, E.; Odériz, I.; Martínez, M.L.; Silva, R. Measurements and modelling of small-scale processes of vegetation preventing dune erosion. *J. Coast. Res.* **2017**, *77* (Suppl. 1), 19–27. [CrossRef]

56. van Puijenbroek, M.E.; Limpens, J.; de Groot, A.V.; Riksen, M.J.P.M.; Gleichman, M.; Slim, P.A.; van Dobben, H.F.; Berendse, F. Embryo dune development drivers: Beach morphology, growing season precipitation, and storms. *Earth Surf. Process Landf.* **2017**, *42*, 1733–1744. [CrossRef]
57. Feagin, R.A.; Furman, M.; Salgado, K.; Martinez, M.L.; Innocenti, R.A.; Eubanks, K.; Figlus, J.; Huff, T.P.; Sigren, J.; Silva, R. The role of beach and sand dune vegetation in mediating wave run up erosion. *Estuarine Coast. Shelf Sci.* **2019**, *219*, 97–106. [CrossRef]
58. Feagin, R.A.; Innocenti, R.A.; Bond, H.; Wengrove, M.; Huff, T.P.; Lomonaco, P.; Tsai, B.; Puleo, J.; Pontiki, M.; Figlus, J.; et al. Does vegetation accelerate coastal dune erosion during extreme events? *Sci. Adv.* **2023**, *9*, eadg7135. [CrossRef] [PubMed]
59. Hayes, M.O.; Moslow, T.F.; Hubbard, D.K. *Beach Erosion in South Carolina*; Coastal Research Division, Department of Geology, University of South Carolina: Columbia, SC, USA, 1978; p. 99.
60. Tides & Currents: Isle of Palms Pier, SC–Station ID 8665494. Available online: https://tidesandcurrents.noaa.gov/stationhome.html?id=8665494 (accessed on 24 July 2020).
61. Kana, T.W. Beach erosion during minor storms. *J. Waterw. Port Coast. Ocean Div.* **1977**, *103*, 505–518. [CrossRef]
62. CSC (Coastal Science & Engineering). *Final Report 2018 Beach Restoration Project City of Isle of Palms*; Technical Report #CSE–2453FR; CSE: Columbia, SC, USA, 2018; p. 57.
63. Tereszkiewicz, P.A.; Ellis, J.T.; Gould, H. Introducing a cost-effective method to assess beach-dune dynamics using existing infrastructure. *J. Coast. Conserv.* **2019**, *23*, 563–618. [CrossRef]
64. Ferguson, J.B. Using Aeolian Depositional Lab Times to Relate Dune Vegetation and Topographic Change. Master's Thesis, University of South Carolina, Columbia, SC, USA, 2020; 74p.
65. Harris, M.E.; Ellis, J.T.; Barrineau, C.P. Evaluating the geomorphic response from sand fences on dunes impacted by hurricanes. *Ocean Coast. Manag.* **2020**, *193*, 105247. [CrossRef]
66. Harris, M.E. Integrated Coastal Science and Dune Management: A South Carolina Perspective. Ph.D. Thesis, Department of Geography, University of South Carolina, Columbia, SC, USA, 2024; 204p.
67. Avila, L.A.; Stewart, S.R.; Berg, R.; Hagen, A.B. *Hurricane Dorian (AL052019)*; National Hurricane Center Tropical Cyclone Report; National Oceanic and Atmospheric Administration: Washington, DC, USA, 2020; 74p.
68. NOAA (National Oceanic and Atmospheric Administration). National Data Buoy Center Continuous Wind Data: Charleston River Cooper Entrance, SC, August–September 2019. Available online: https://www.ndbc.noaa.gov/station_page.php?station=chts1 (accessed on 5 October 2019).
69. NWS (National Weather Service). Charleston Daily Precipitation Data. Available online: https://www.weather.gov/chs/climate (accessed on 3 November 2019).
70. NOAA (National Oceanic and Atmospheric Administration). National Data Buoy Center Continuous Wave Data: Edisto Buoy, SC, August–September 2019. Available online: https://www.ndbc.noaa.gov/station_page.php?station=41004 (accessed on 5 October 2019).

Disclaimer/Publisher's Note: The statements, opinions and data contained in all publications are solely those of the individual author(s) and contributor(s) and not of MDPI and/or the editor(s). MDPI and/or the editor(s) disclaim responsibility for any injury to people or property resulting from any ideas, methods, instructions or products referred to in the content.